Inventory changes in anthropogenic carbon from 1997–2003 in the Atlantic Ocean between 20°S and 65°N

Reiner Steinfeldt,[1] Monika Rhein,[1] John L. Bullister,[2] and Toste Tanhua[3]

Received 25 July 2008; revised 17 February 2009; accepted 1 April 2009; published 22 July 2009.

[1] The oceans absorb and store a significant portion of anthropogenic CO_2 emissions, but large uncertainties remain in the quantification of this sink. An improved assessment of the present and future oceanic carbon sink is therefore necessary to provide recommendations for long-term global carbon cycle and climate policies. The formation of North Atlantic Deep Water (NADW) is a unique fast track for transporting anthropogenic CO_2 into the ocean's interior, making the deep waters rich in anthropogenic carbon. Thus the Atlantic is presently estimated to hold 38% of the oceanic anthropogenic CO_2 inventory, although its volume makes up only 25% of the world ocean. Here we analyze the inventory change of anthropogenic CO_2 in the Atlantic between 1997 and 2003 and its relationship to NADW formation. For the whole region between 20°S and 65°N the inventory amounts to 32.5 ± 9.5 Petagram carbon (Pg C) in 1997 and increases up to 36.0 ± 10.5 Pg C in 2003. This result is quite similar to earlier studies. Moreover, the overall increase of anthropogenic carbon is in close agreement with the expected change due to rising atmospheric CO_2 levels of 1.69% a^{-1}. On the other hand, when considering the subpolar region only, the results demonstrate that the recent weakening in the formation of Labrador Sea Water, a component of NADW, has already led to a decrease of the anthropogenic carbon inventory in this water mass. As a consequence, the overall inventory for the total water column in the western subpolar North Atlantic increased only by 2% between 1997 and 2003, much less than the 11% that would be expected from the increase in atmospheric CO_2 levels.

Citation: Steinfeldt, R., M. Rhein, J. L. Bullister, and T. Tanhua (2009), Inventory changes in anthropogenic carbon from 1997–2003 in the Atlantic Ocean between 20°S and 65°N, *Global Biogeochem. Cycles*, *23*, GB3010, doi:10.1029/2008GB003311.

1. Introduction

[2] Since approximately 40% of the anthropogenic emissions of CO_2 is stored in the ocean [*Sabine et al.*, 2004], knowledge of the oceanic uptake and resulting inventory increase of anthropogenic CO_2 is important in understanding the global carbon budget. Direct measurements of pCO_2 and dissolved inorganic carbon (DIC), however, only provide information on the total ocean-atmosphere CO_2 fluxes and oceanic carbon concentrations. The anthropogenic carbon (C_{ant}) increase in the ocean resulting from the rising atmospheric CO_2 is small relative to the large background DIC signal in the ocean and has to be inferred by indirect methods. One common technique, the ΔC^* method [*Gruber et al.*, 1996], involves making corrections for biogeochemical processes (remineralization, calcium carbonate dissolution) and initial CO_2 disequilibrium to estimate the preindustrial carbon concentration and to separate the anthropogenic fraction from the measured total. This method, however, infers only low concentrations of anthropogenic carbon in the deep overflow waters, even though transient tracers show that these waters are recently ventilated, suggesting a significant burden of C_{ant} [*Tanhua et al.*, 2007]. Here we use the transit time distribution (TTD) method [*Waugh et al.*, 2006], which shows the expected elevated levels of C_{ant} in these water masses.

[3] Compared to *Waugh et al.* [2006], we apply a slightly different approach, as the ratio of the TTD parameters Γ (mean age) and Δ (width) is not assumed to have a constant value of 1 and is allowed to vary spatially. This improved TTD method is elaborated in section 2. On the basis of these optimized TTD parameters, the inventory of anthropogenic carbon in the Atlantic between 20°S and 65°N is calculated for the years 1997 and 2003. The TTD parameters are inferred from CFC observations from the late WOCE period, CLIVAR and German national programs. The inventories presented here are thus an update of previous studies, which are mainly based on data from the 1990s. The errors of the computed C_{ant} inventories are discussed in detail in section 4. Special focus is on the air-sea CO_2 disequilibrium, which is assumed to be constant when applying the TTD method. In order to investigate the variability of water mass formation on the oceanic C_{ant}

[1] Institut für Umweltphysik, Universität Bremen, Bremen, Germany.
[2] Pacific Marine Environmental Laboratory, NOAA, Seattle, Washington, USA.
[3] Marine Biogeochemie, Leibniz-Institut für Meereswissenschaften an der Universität Kiel, Kiel, Germany.

0886-6236/09/2008GB003311$12.00

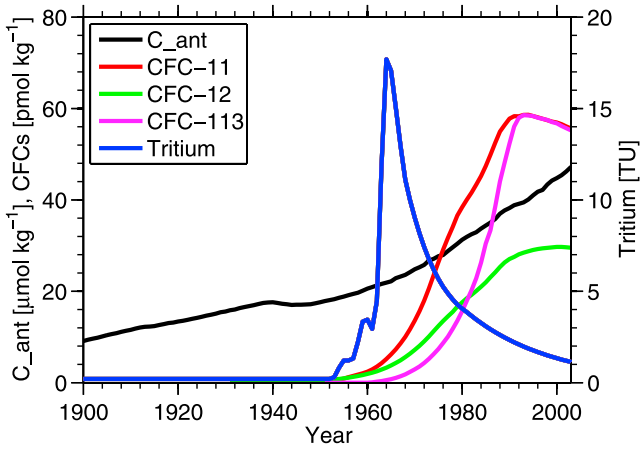

Figure 1. Time history for CFCs, tritium, and anthropogenic carbon in the surface mixed layer. CFC and CO_2 are calculated assuming solubility equilibrium for a temperature of 3.0°C and salinity S = 34.9, characteristic for North Atlantic Deep Water. To fit a common scale in this figure, CFC-11 and CFC-12 are multiplied by 10, and CFC-113 is multiplied by 100.

storage, in section 5 the C_{ant} inventory is calculated for all components of North Atlantic Deep Water ((Upper) Labrador Sea Water, North East Atlantic Deep Water, Denmark Strait Overflow Water) over the subpolar northwestern Atlantic.

2. TTD Method

2.1. Introduction

[4] The TTD method is based on the assumption that any water parcel in the ocean interior consists of many infinitesimal fluid elements of different ages or transit times (time elapsed since the fluid element left the surface mixed layer). The distribution or probability density function of these different ages is the TTD $\mathcal{G}$. The concentration of any dissolved constituent in the ocean interior $C(\mathbf{x}, t)$ is given by the convolution integral of the TTD $\mathcal{G}(\mathbf{x}, \tau)$ and the (time-dependent) concentration of the constituent in the surface mixed layer $C^0(t)$:

$$C(\mathrm{x}, t) = \int_0^\infty C^0(t-\tau)\mathcal{G}(\mathbf{x}, \tau)\, d\tau' \qquad (1)$$

In several earlier ocean studies, the TTD $\mathcal{G}(\mathbf{x}, \tau)$ is approximated by an inverse Gaussian distribution [*Waugh et al.*, 2004, 2006] with two parameters, the mean age (first moment) Γ and the width (proportional to the second moment) Δ:

$$\mathcal{G}(\tau, \Gamma, \Delta) = \sqrt{\frac{\Gamma^3}{4\pi\Delta^2\tau^3}} \exp\left(\frac{-\Gamma(\tau-\Gamma)^2}{4\Delta^2\tau}\right). \qquad (2)$$

where τ is the transit time or age of the water. $\mathcal{G}(\tau, \Gamma, \Delta)$ is a solution to the one-dimensional advection diffusion equation with constant velocity and diffusivity.

[5] The mixed layer concentration of anthropogenic carbon and the transient tracers CFC-11, CFC-12, CFC-113, and tritium as a function of time are shown in Figure 1. The tritium curve for the North Atlantic Ocean [*Dreisigacker and Roether*, 1978] is continued assuming radioactive decay after 1978. CFCs are calculated from their atmospheric mixing ratios [*Walker et al.*, 2000] and their solubility [*Warner and Weiss*, 1985]. C_{ant} is computed from the atmospheric CO_2 mixing ratios [*Neftel et al.*, 1994; *Keeling and Whorf*, 2005] CO_2 solubility [*Weiss*, 1974], and equilibrium inorganic carbon chemistry [*Dickson and Goyet*, 1994]. Alkalinity is determined from θ and salinity S according to *Lee et al.* [2006]. $C_{ant}(t)$ is defined as $C_{eq}(t) - C_{eq}^{preind}$, which implies that a (possible) disequilibrium of inorganic carbon in the mixed layer remains constant with time. C_{eq}^{preind} denotes the equilibrium inorganic carbon concentration at preindustrial time, i.e., before the year 1800.

2.2. Determination of TTD Parameters

[6] Equation (1) can also be used to constrain the TTD parameters Γ and Δ from observed tracer concentrations $C(\mathbf{x}, t)$. For a given concentration of CFC-11, the concentration of a second tracer such as CFC-113, tritium, or C_{ant} depends on the ratio of the TTD parameters Γ and Δ. This can be exploited to constrain the values of both parameters. Because of differences in their characteristic time histories and the impacts of mixing on their concentration in the subsurface ocean, typically, CFC-113 concentrations increase with increasing Δ/Γ ratio, whereas tritium and C_{ant} decrease. These variations are more pronounced for smaller CFC-11 concentrations, i.e., in older water (Figure 2). Thus in the deep ocean, where strong mixing of young and old waters occurs (which implies large Δ/Γ ratios), assuming a too low value of Δ/Γ (i.e., unity) would lead to an overestimation of C_{ant}. The high tritium concentrations for CFC-11 < 1 pmol kg^{-1} and $\Delta/\Gamma \approx 0$ correspond to an almost undiluted advection of the tritium peak from the 1960s. As this has not been observed in the deep northeastern Atlantic [*Fleischmann et al.*, 2001], a Δ/Γ ratio of 0 seems unrealistic. The variation of all three tracers with Δ/Γ is large for $0 < \Delta/\Gamma < 1$ and small for $\Delta/\Gamma > 2$. This implies that even with simultaneous measurements of CFC-11, CFC-113, and tritium it is not possible to distinguish between Δ/Γ values that are larger than 2. On the other hand, this is not a significant problem for the calculation of C_{ant} from the TTDs, since the C_{ant} concentration for a given CFC-11 shows only small changes for $\Delta/\Gamma > 2$.

[7] If only one tracer is available (e.g., CFC-11), a large range of Γ-Δ pairs is possible to fulfill equation (1). This is illustrated in Figure 3a, where four Γ-Δ pairs are derived from a CFC-11 value of 0.57 pmol kg^{-1} observed in 2000 at 16°N at the western boundary [*Steinfeldt et al.*, 2007]. The shown TTDs have Δ/Γ ratios of 0, 0.5, 1, and 2, but principally for each prescribed Δ/Γ ratio a TTD can be derived. For a Δ/Γ ratio of 0 the TTD is a δ function, and the mean age equals the concentration age. With increasing Δ/Γ the TTDs become broader, and the maximum is shifted toward younger ages. CFC-12 data together with CFC-11 does not lead to an appreciable reduction of the allowed

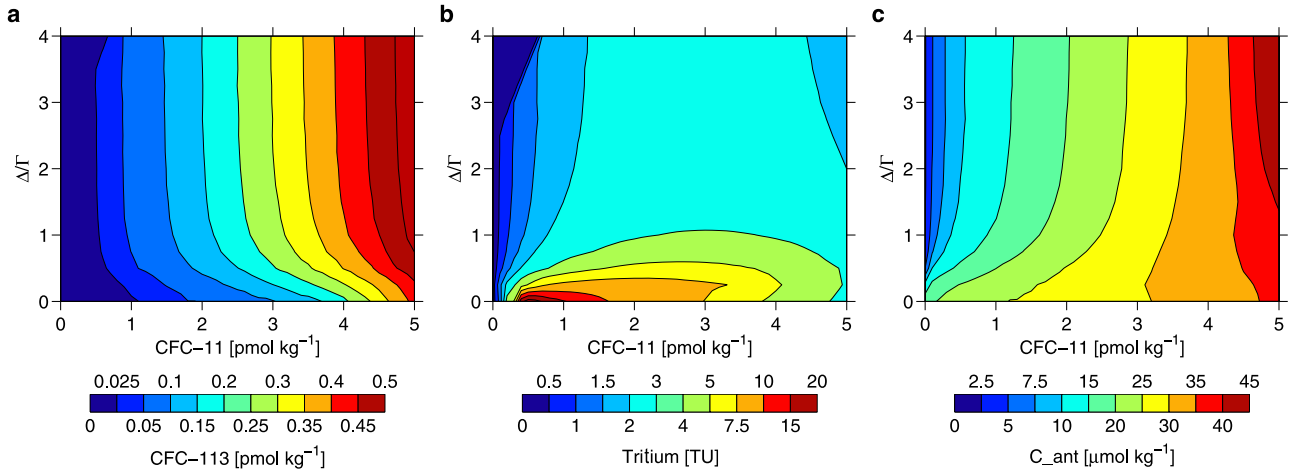

Figure 2. Concentrations of (a) CFC-113, (b) tritium, and (c) C_{ant} as a function of the CFC-11 concentration and the parameter ratio Δ/Γ. All tracer values are calculated for the year 2000 with characteristic NADW properties and solubility equilibrium of tracers with the atmosphere.

Γ-Δ range, as the atmospheric time history of both tracers is quite similar.

[8] CFC-11, CFC-113, and tritium data collected between 1994 and 2005 are used to infer the Δ/Γ ratio. The data from the whole time period are assembled, as CFC-113 and tritium data are sparse. We thus assume that the Δ/Γ ratio remains constant with time, whereas the absolute values of Δ and Γ may change. The tracer data are interpolated isopycnally within 23 density layers, then for each layer the Δ/Γ ratio is determined and gridded onto a 0.5° × 0.5° between 20°N and 65°N using a terrain following interpolation scheme. The range of the Δ/Γ ratio is restricted to 0.5, 1, and 2. Larger ratios cannot be derived using CFC-113 and tritium data as illustrated above, and the measurement error of the small CFC-113 concentrations as well as the methodological error (the real shape of the TTD may divide from the prescribed Inverse Gaussian form) makes a finer resolution of the Δ/Γ ratio unrealistic.

[9] As an example for the spatial distribution of the Δ/Γ ratios in deep water, the core layer of Labrador Sea Water is discussed (Figure 3b). A southward increase of Δ/Γ is obvious, and this increase is more pronounced in the

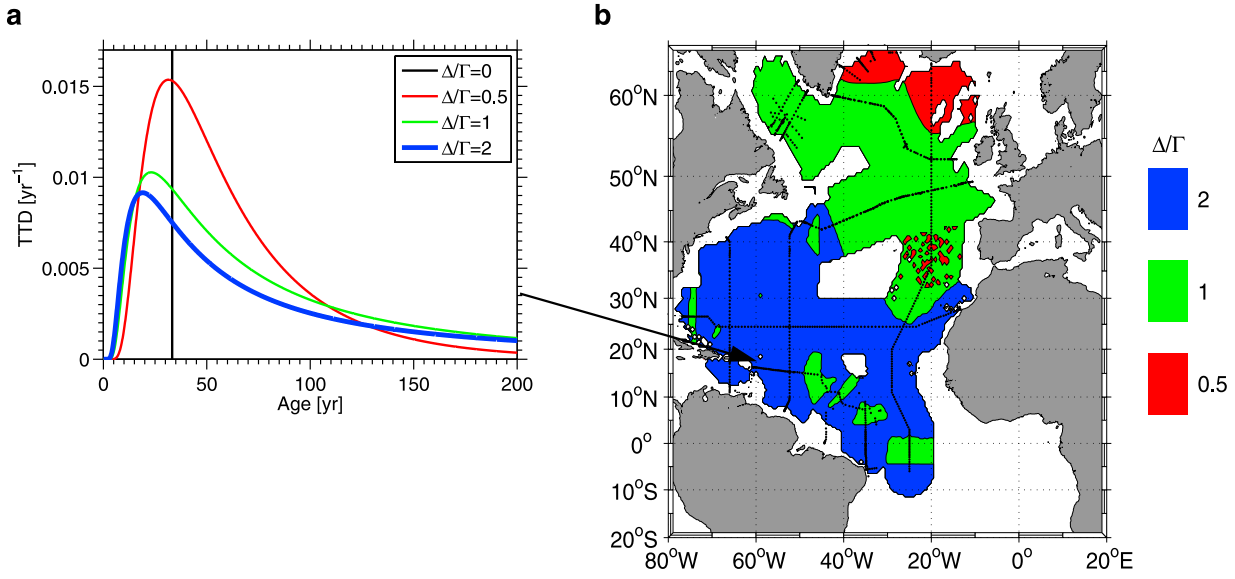

Figure 3. (a) Transit time distributions (TTD) for the core layer of Labrador Sea Water at 16°N/61°W derived from CFC-11 observations in 2000 and different Δ/Γ ratios. The TTD for the optimal Δ/Γ ratio (i.e., 2) is highlighted in bold. (b) Map of Δ/Γ ratios inferred from simultaneous CFC-11/CFC-113 and CFC-11/tritium observations for the core layer of Labrador Sea Water (LSW) (2000 m depth).

Table 1. Water Masses

Approximate Depth Range (m)[a]	Subpolar North Atlantic	Subtropical/Tropical Atlantic
0–500	SPMW	CW
500–1000	SPMW	IW
1000–1500	ULSW	ULSW
1500–2500	LSW	LSW
2500–3500	NEADW	NEADW
3500–4500	DSOW	DSOW
4500–bottom		AABW

[a]The exact vertical extent of the water masses at each station is calculated from the density. For the subpolar and the subtropical/tropical region, different density boundaries are applied [*Stramma et al.*, 2004; *Rhein et al.*, 2005; *Steinfeldt et al.*, 2007]. The North Atlantic Deep Water (NADW) comprises the water masses Upper Labrador Sea Water (ULSW), Labrador Sea Water (LSW), North East Atlantic Deep Water (NEADW), and Denmark Strait Overflow Water (DSOW). CW, Central Water. SPMW, Subpolar Mode Water. IW, Intermediate Water. AABW, Antarctic Bottom Water.

western basin. These regional variations of Δ/Γ are characteristic also for the other NADW layers. The large Δ/Γ ratios in the western tropical Atlantic result in asymmetric TTDs with their maxima at young ages and a long tail (Figure 3a). Such a form of the TTDs can be interpreted as a consequence of strong mixing of young NADW advected along the western boundary with older water present in the interior of the subtropical and tropical Atlantic. East of the Caribbean at 16°N, for example, the maximum of the TTD in the Labrador Sea Water (LSW) layer (about 2000 m depth) occurs at an age of about 15 years if the $\Delta/\Gamma = 2$ derived from the tracer observations is applied. For smaller Δ/Γ ratios, the maximum of the TTD occurs at higher ages (Figure 2b). The 15 years from the $\Delta/\Gamma = 2$ case are in qualitative agreement with other estimations of the spreading time of NADW from the Labrador Sea toward the tropics [*Steinfeldt and Rhein*, 2004; *Steinfeldt et al.*, 2007]. The fraction of young, CFC carrying water has been estimated to be about 25%, which is confirmed in this study, as the fraction of water with ages younger than 50 years (older waters are almost free of CFCs) is about 30% for the TTD with $\Delta/\Gamma = 2$.

3. Anthropogenic Carbon Inventories

3.1. Introduction

[10] The inventory of anthropogenic carbon of the Atlantic is calculated from CFC-11 as follows: The CFC-11, salinity, and potential temperature profiles are integrated isopycnally as described in section 2.2, then C_{ant} is calculated via equation 1 for TTDs with Δ/Γ ratios between 0 and 2. The quantities for each isopycnal layer (C_{ant} and layer thickness) are interpolated horizontally in the same way as Δ/Γ ratios, and then the inventory of anthropogenic carbon for different water masses (see Table 1) is computed for the years 1997 and 2003. As both the TTD parameters and the thicknesses of the isopycnal layers may change with time, in an idealized case, only data from the specific year should be used. This is, however, only possible for the subpolar North Atlantic, were the data coverage in 1997 and 2003 is sufficient to provide an excellent basis for the horizontal interpolation. For observations in the subtropics and tropics, the time frame is extended to ±1 year and to ±3 years, respectively. The total number of CFC samples is about 54,600 collected at 3890 profiles.

[11] The anthropogenic carbon inventory of the different water masses in 1997 is shown in Figure 4 as a function of Δ/Γ. Using at each grid point the Δ/Γ value inferred from CFC-11, CFC-13, and tritium, the resulting "optimal" inventory is calculated and highlighted in Figure 4. This optimal inventory is close to the $\Delta/\Gamma = 1$ case, slightly higher for the (Upper) Labrador Sea Water, and slightly lower for the DSOW and AABW. Regionally, the differences between the $\Delta/\Gamma = 1$ and the variable Δ/Γ ratio can be larger, as is seen from Figure 3b for the LSW core layer. The large regions in the tropical Atlantic where $\Delta/\Gamma = 2$ contain old water with very low C_{ant} concentrations. The LSW C_{ant} inventory is thus dominated by the subpolar regions, where the optimal Δ/Γ ratio is 1 or 0.5.

[12] For the intermediate, central, and mode water masses overlying the NADW, the tritium and CFC-113 data are not suited to improve the estimates of Δ/Γ in this study, since CFC-113 is not stable in these warmer waters, and the surface concentrations of tritium vary over the extended source regions. A parameter ratio of $\Delta/\Gamma = 1$ is thus used for all water masses located above the NADW. For the C_{ant} calculation, this simplified assumption for the upper water masses has a smaller effect than for NADW, since the dependence of C_{ant} on the Δ/Γ ratio is small for recently ventilated waters with high CFC-11 concentrations (Figures 2 and 4). The inventory integrated over the whole region from 20°S to 65°N adds up to 32.5 ± 9.5 Petagram carbon (Pg C) in 1997. Contrary to the other oceans, almost half of this inventory is contained in the deep and bottom waters (Figure 4), which leads to the high C_{ant} inventory per area of the Atlantic compared to the Pacific or Indian Ocean.

[13] The important role of NADW for the C_{ant} storage of the Atlantic is reflected in the column inventory (Figure 5): This is characterized by a decrease from north to south along the NADW spreading pathways, whereas the zonal change is smaller. The maximum occurs in the Labrador Sea, where the locally formed Labrador Sea Water (LSW)

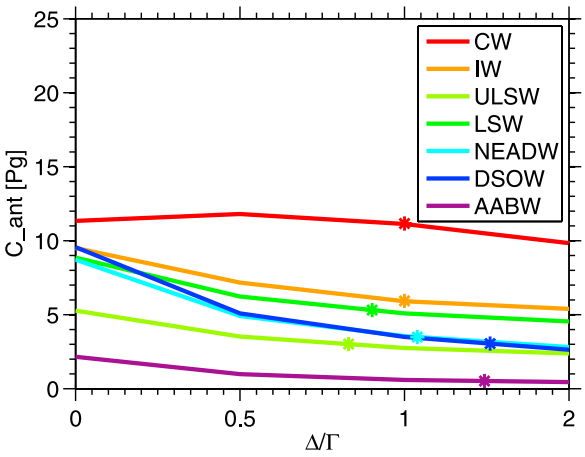

Figure 4. C_{ant} inventory for different water masses as a function of the Δ/Γ ratio in 1997. The inventory for the optimal Δ/Γ values determined from CFC-11/CFC-113, and CFC-11/tritium observations are marked by asterisks.

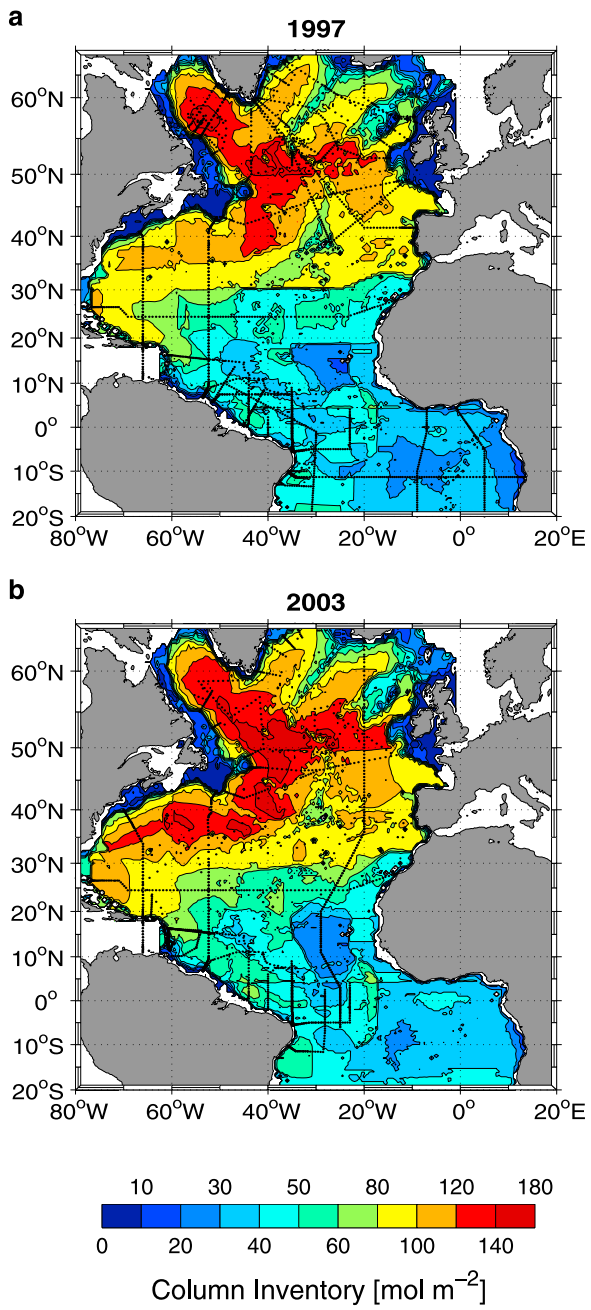

Figure 5. C_{ant} column inventory for (a) 1997 and (b) 2003. The black dots denote measurements.

and lighter Upper LSW (ULSW) contribute to the high column inventory. Additionally, the overflow waters from the Nordic Seas pass through this region. The NADW is exported toward the south mainly along the western boundary. LSW and ULSW additionally spread into the eastern Atlantic via the fracture zones in the Mid-Atlantic Ridge. As the water becomes older during its spreading, the C_{ant} concentrations decrease downstream.

3.2. Temporal Increase of C_{ant}

[14] The inventory for 2003, calculated in the same way as for 1997, but with CFC data collected around the year 2003 (in 2003 in the North Atlantic, between 2000 and 2006 in the tropical Atlantic), is 36.0 ± 10.5 Pg C. The column inventories increased almost overall; one exception is the convection region in the central Labrador Sea, where no maximum of the column inventory can be found in 2003 (Figure 5).

[15] In order to investigate the reason for the C_{ant} changes between 1997 and 2003, the C_{ant} increase due to the rising atmospheric CO_2 levels has to be distinguished from oceanic C_{ant} changes due to the variability of water mass formation and circulation. This is done by recalculating C_{ant} for 2003 with the TTDs and layer thicknesses from the 1997 data. The resulting C_{ant} inventories can be interpreted as a forecast for 2003, assuming a steady state ocean. The difference between this forecast and the real 2003 C_{ant} values (derived from 2003 CFC data and layer thicknesses) is a measure for the impact of the oceanic variability on the C_{ant} storage.

[16] Another possibility is to exploit the almost exponential time history of atmospheric CO_2 and C^0_{ant} in the ocean mixed layer for the period after 1850: $C^0(t) = Ae^{\lambda t}$, $C^0(t_2) = C^0(t_1)e^{\lambda(t_2-t_1)}$ (Figure 6). Then the concentration of C_{ant} at times t_1 and t_2 is simply related via

$$C(t_2) = e^{\lambda(t_2-t_1)} \int_0^\infty C^0(t_1)\mathcal{G}(x,\tau)\,d\tau' = e^{\lambda(t_2-t_1)}C(t_1) \qquad (3)$$

The factor λ is 59.38 a^{-1} which corresponds to an increase rate of 1.69% a^{-1} if C^0_{ant} is calculated for characteristic NADW properties (Figure 6). The results for the Atlantic anthropogenic carbon inventory for 2003 are 36.0 Pg C for both cases, i.e., using the forecast from the TTDs in 1997 or the annual increase rate from equation (3). It is thus shown that the error using equation (3) due to the deviations of C^0_{ant} from the exponential curve is small. This demonstrates that the concept of a transient steady state

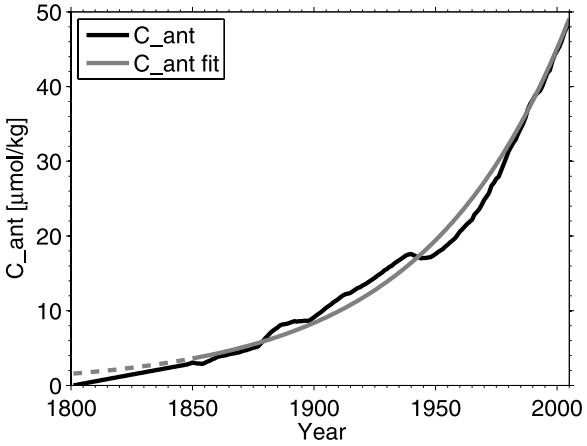

Figure 6. (solid black curve) Time history of C^0_{ant} in the surface mixed layer calculated as in Figure 1 and (solid gray curve) exponential fit for the time after 1850. (dashed gray curve) The exponential fit is extrapolated between 1800 and 1850.

[*Gammon et al.*, 1982] may be applied, as was done by *Tanhua et al.* [2007] to derive total C^0_{ant} concentrations from eLMR results. This may not work, however, in regions of strong variability as the subpolar North Atlantic, especially the Labrador Sea. There, quite a large discrepancy between the C^0_{ant} inventory in 2003 and the forecast from the TTDs in 1997 exist, which is discussed in section 5.

[17] The overall C^0_{ant} inventory increased between 1997 and 2003 as would be expected from the atmospheric CO_2 increase and is unaffected from ocean variability. The annual growth rate of C^0_{ant} of 1.69%, multiplied with the C_{ant} inventory yields an annual increase rate of 0.55 Pg C a^{-1}.

[18] For Labrador Sea Water alone, the uptake (neglecting the small export at 20°S) is 0.09 Pg C a^{-1} or 0.56 Pg C between 1997 and 2003. This illustrates that even a complete shutdown of LSW formation would only lead to a small reduction of the C_{ant} inventory in 2003 of 0.56 Pg C compared to the case of a steady state ocean. This difference is too small to show up in the total inventory. On the other hand, the decrease of the column inventories in the Labrador Sea between 1997 and 2003 strongly suggests an influence of ocean variability on the C_{ant} inventory. Before analyzing these changes in the northwestern region in more detail, an error analysis is carried out, which allows the detection of significant changes in the regional C_{ant} inventories.

4. Error Analysis

[19] For the computation of the C_{ant} inventories, two principal sources of error can be distinguished. First, the inventory computed from gridded data includes an interpolation and extrapolation error. Second, the C_{ant} concentrations are estimations depending on the method used to infer C_{ant}, in this case the TTD method.

4.1. Interpolation Error

[20] The interpolation error of the C_{ant} inventory is estimated by comparing the gridded values of different subsets to the grid from the full data set and is about 2%. In some regions, such as the eastern Atlantic south of the equator in 2003, no data are present. Such large data gaps are not filled by the interpolation scheme. On the other hand, leaving out these areas would leave to a large underestimation of the total inventory, so data were extrapolated to fill the gaps. Almost all regions are covered either by 1997 or by 2003 data. It is therefore assumed that the percentage relative to the whole inventory in regions without data in 1997 or 2003 is the same as in the other year. This corresponds to the method "Added %" given by *Kieke et al.* [2006]. These extrapolated inventories make up about 20% of the whole inventory. The mean inventory increase between 1997 and 2003 is 11%. If it is assumed that for the data gaps the real inventory difference between 1997 and 2003 may vary between 0 and 22% (i.e., between no increase and twice the mean increasing rate), the resulting error of the total inventory from the extrapolation is 2.2% at maximum. The total error from interpolation and extrapolation thus amounts to 3.0% (the quadratic sum of the individual errors).

4.2. Methodological Errors

4.2.1. DIC Disequilibrium

[21] As outlined above, the TTD method relies on the assumption of a constant DIC disequilibrium over time. A time history for this disequilibrium from 1800 to 2003 cannot be inferred from observations. Here we will at least investigate the DIC disequilibrium at the time of water mass formation for 1997 and 2003 data in the North Atlantic. The disequilibrium can be inferred from measured DIC data and the TTDs inferred in this study. Similar to *Gruber et al.* [1996] for the determination of ΔC^*, the DIC originating from the remineralization of organic matter and from the dissolution of calcium carbonate is subtracted from the measured DIC as well as the DIC equilibrium concentration at the time of water mass formation. The latter is given by the convolution integral of the TTD with the equilibrium DIC time history, which is the sum of the equilibrium preindustrial carbon and the C^0_{ant} time history from Figure 1. The resulting quantity is the DIC disequilibrium DIC_{diseq} at the time of water mass formation:

$$\begin{aligned} DIC_{diseq} &= DIC - DIC_{eq}(1780) - C_{ant} - 117/170 * AOU \\ &\quad - 0.5 * (Alk - Alk_0 + 16/170 * AOU). \end{aligned}$$

$DIC_{eq}(1780)$ is the preindustrial equilibrium oceanic DIC concentration, Alk_0 is the preformed alkalinity computed according to *Lee et al.* [2006], AOU is the apparent oxygen utilization, and the factors 117/170 and 16/170 are the $C/-O_2$ and $N/-O_2$ ratios determined by *Anderson and Sarmiento* [1994]. Since a number of different quantities must be measured at the same location to infer DIC_{diseq}, the number of available data is much less than for CFCs alone. Therefore, no horizontal interpolation is performed on this quantity. Isopycnal mean profiles for DIC_{diseq} are considered instead. These are shown for the Meteor cruises over the subpolar North Atlantic in 1997, M39/2, M39/3, and M39/4 (summarized as M39), and M59/2 in 2003 in Figure 7. Above the NADW, DIC_{diseq} increased between 1997 and 2003. The increase in the surface layers reaches up to 10 μmol kg^{-1}(equivalent to a change in pCO_2 of about 20 ppm). This reflects the findings of *Lefèvre et al.* [2004] and *Schuster and Watson* [2007], that the surface ΔpCO_2, defined as atmospheric pCO_2 minus sea surface pCO_2, decreased. Over the NADW range, DIC_{diseq} remains almost constant between 1997 and 2003. The increase at the lower boundary of DSOW is not significant because of the limited number of data (no standard deviation was calculated for the 2003 data for densities $\sigma_\theta > 27.9$ kg m^{-3} as the number of profiles is less than 3). The maximal temporal change of DIC_{diseq} between 1997 and 2003 is 10 μmol kg^{-1} in the surface and mode water, which corresponds to about 20% of the C_{ant} concentration.

[22] Over the whole period from 1800 to 2003, the variation of DIC_{diseq} could even be larger than the 20% observed between 1997 and 2003. *Terenzi et al.* [2007] find that the saturation of C_{ant} in the LSW outcrop region decreases with time and is between 18 and 40% at present. Their study, however, uses only two parameters for the mean TTD of the whole LSW volume, whereas here we use two parameters at each profile for each isopycnal level,

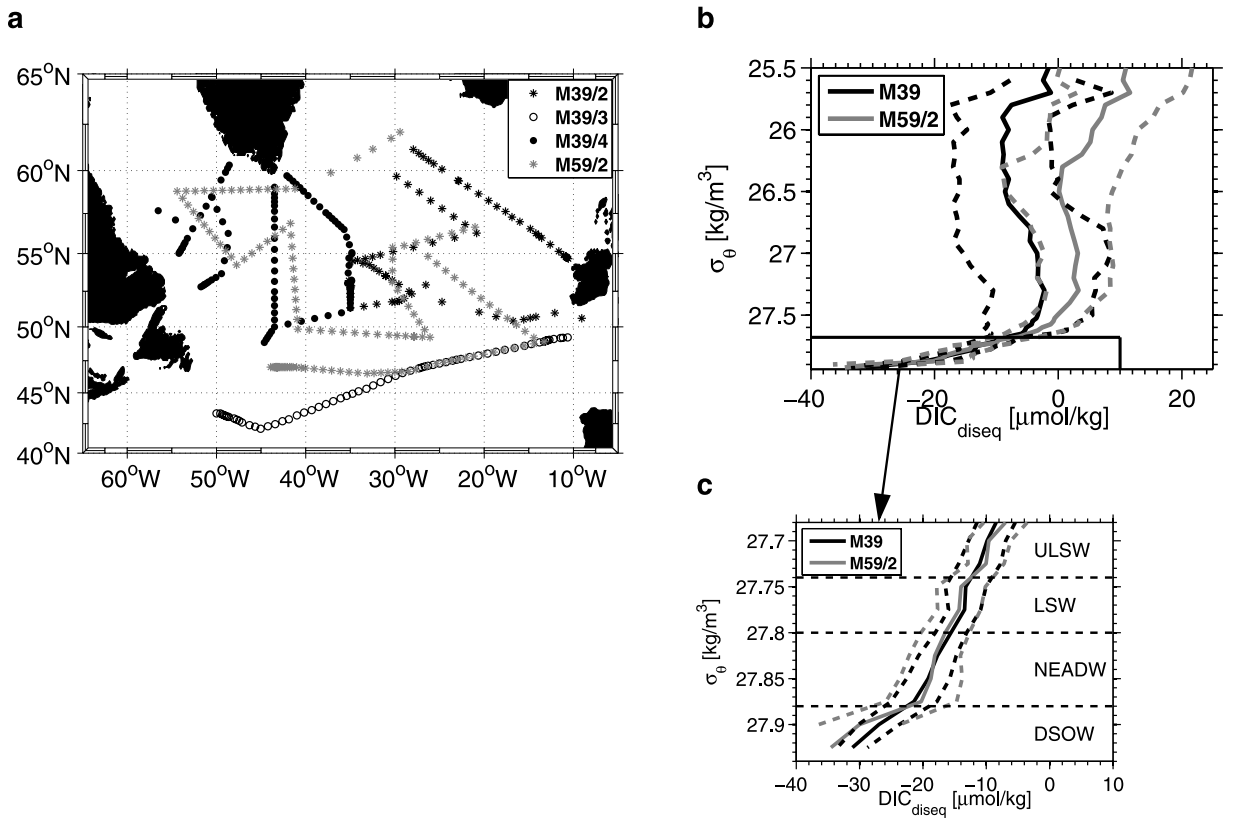

Figure 7. (a) Cruise map of Meteor M39/2, M39/3,and M39/4 (1997) and M59/2 (2003). (b) Mean profiles of DIC_{diseq} for 1997 (M39) and 2003 (M59/2) (for details, see section 4.2.1); the dashed lines denote ± one standard deviation around the mean profiles. (c) Same as Figure 7b, but enlarged representation for the density range of NADW.

which is probably more realistic. This result is also in contrast with observations from the North Atlantic [*Omar and Olsen*, 2006; *Corbière et al.*, 2006; *Schuster and Watson*, 2007], which demonstrate that the oceanic partial pressure of CO_2 over the North Atlantic during the last decades increased even stronger than the atmospheric CO_2.

[23] A part of the observed DIC changes is due to the variability of natural carbon which would arise also under constant atmospheric CO_2 levels. These variations of natural carbon do not influence C_{ant}; thus the temporal change of the C^0_{ant} saturation is smaller than the variability of DIC_{diseq}, which implies that the C^0_{ant} changes are less than 20% for the period 1997–2003. As a rough estimation, we take the value of 20% as the temporal change of DIC_{diseq} and thus the error of C_{ant} arising from temporal changes of the DIC disequilibrium.

4.2.2. CFC Disequilibrium

[24] Another assumption used here to infer the TTD parameters from the CFC concentration is the constant CFC saturation in the mixed layer, which is assumed to be between 65% (bottom waters) and 100% (surface waters), depending on the isopycnal layer. Also this saturation is likely to vary with time [*Tanhua et al.*, 2008]. The influence of the CFC concentration on anthropogenic

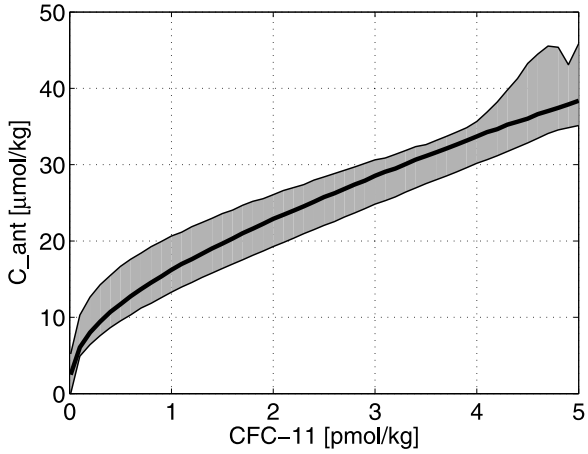

Figure 8. C_{ant} as a function of CFC-11. The shaded area indicates the range of C_{ant} resulting from deviations of the CFC-11 concentration by ±10% (due to oversaturation/undersaturation or measurement errors). In this example, C_{ant} is calculated from TTDs with a Δ/Γ ratio of one, but other Δ/Γ ratios yield similar ranges of C_{ant} concentrations when CFC-11 varies by ±10%. All calculations are for a potential temperature θ of 3.0°C and a salinity S of 34.9.

carbon is illustrated in Figure 8. The thick line shows the CFC-11 – C_{ant} relation for $\Delta/\Gamma = 1$ in 1997. The gray shaded area is the range of C_{ant} resulting from CFC-11 concentrations varying by ±10%, which is a realistic uncertainty due to a varying degree of saturation [*Tanhua et al.*, 2008]. Surprisingly, the resulting C_{ant} concentration varies only by ±5%, except for the case of high CFC-11 concentrations. Atmospheric CFC-11 mixing ratios have been nearly constant since the beginning of the 1990s. Thus small changes of CFC-11 in young water yield large changes in the derived age and TTD parameters. Measurement errors, normally less than 2%, falsify the inventory estimate in the same way as an incorrect surface saturation. Both uncertainties thus yield an error for C_{ant} of about 5.5% for older and 10% for young water.

4.2.3. C_{ant} in CFC-Free Water

[25] The quantification of C_{ant} in old waters with zero or very low CFC-11 concentrations is also a source of error. For CFC-free waters (the detection limit of CFC-11 is around 0.005 pmol kg^{-1}), no TTD parameters and no C_{ant} values can be determined by the method presented here, so C_{ant} is also set to zero in this case. This may be an erroneous underestimation, as C_{ant} has been present in the atmosphere and surface water for about 200 years, while CFC-11 (and CFC-12) have been present only for about 50 years. The maximum C_{ant} concentrations for CFC-11 below detection limit derived from the TTD method are in the range of 1.5–2.0 μmol kg^{-1}. Assuming this uncertainty for the whole deep water in the subtropical and tropical Atlantic below ≈2500 m, the resulting inventory error is about 2 Pg C, i.e., about 6% of the whole inventory.

4.2.4. C_{ant} Error due to TTD Parameterization

[26] As illustrated in section 2.2, different ratios of the TTD parameters Δ/Γ lead to different C_{ant} concentrations (Figures 2 and 4). The larger effects of the Δ/Γ ratio on C_{ant} can be found in the deep waters, where the CFC concentrations are relatively low. Besides an error in the estimation of the optimal Δ/Γ ratio, the shape of the TTD is subject to other uncertainties. The functional form for parameterizing the "real" TTDs used here is an inverse Gaussian distribution. This distribution applies for an ocean modeled by one-dimensional, temporal-independent advection diffusion equation, but the real ocean is three-dimensional and not in steady state. The influence of such a "nonanalytic" TTD on the C_{ant} concentration again can only be estimated. It is assumed that the error of C_{ant} due to a nonanalytical shape of the TTD is similar to the variations of the parameters Δ/Γ, which also influences the shape of the TTD. Therefore, the C_{ant} inventory probably is in the range of $0.5 < \Delta/\Gamma < 2$ in Figure 4. This leads to an error of about 20% for the total C_{ant} inventory for the deep water masses. For the younger waters, the exact shape of the TTD has a smaller influence on the C_{ant} inventory in the range of 10% (Figure 4).

4.3. Error of C_{ant} Inventories and Inventory Differences

[27] The total mean error of all the methodological uncertainties is the quadratic sum of the errors estimated in the previous sections, i.e., 29%. For young water, the error due to the TTD shape is smaller, which is compensated by a larger error due to the uncertainty in the CFC saturation. The 29% error is applicable to the total C_{ant} inventory.

[28] If the inventories between 1997 and 2003 are compared, the resulting error is much smaller. Most of the water present in the Atlantic in 2003 has been there already in 1997, as the ventilation time of the Atlantic is much larger than 6 years. Errors from unrealistic DIC and CFC disequilibria for the waters formed before 1997 almost cancel out when considering the inventory difference between 2003 and 1997. Also the shape of the TTDs in most places cannot change dramatically, as the water is only partially exchanged or renewed within 6 years. The errors resulting from these sources of uncertainty thus reduce by a factor of about 10 (i.e., they are only applied to the additional C_{ant} inventory of 11%), when comparing the 1997–2003 inventory changes. For this difference, the interpolation and extrapolation error has to be taken into account for both the 1997 and the 2003 inventory; thus the error for the inventory difference is about 5%.

[29] The inventories presented so far are based on the CFC-11 measurements. The CFC-12 measurements can be used in the same way to infer the TTDs and C_{ant} values. The resulting inventories derived using CFC-12 are 33 Pg C in 1997 and 37 Pg C in 2003, i.e., 1.5–2.8% larger than the inventories based on CFC-11. These small deviations can be explained by measurement errors and a slightly different saturation in the mixed layer of both CFC components.

5. Variability of C_{ant} Inventory in the Subpolar North Atlantic

[30] During the last decade, the ocean circulation in the North Atlantic, especially the water mass formation in the Labrador Sea, underwent dramatic changes [*Lazier et al.*, 2002; *Kieke et al.*, 2007]. The large amount of CFC data from the northwestern subpolar Atlantic allows calculation of the regional C_{ant} inventory for 1997, 1999, 2001, and 2003. The increase of C_{ant} due to rising atmospheric CO_2 (1.69% per year, see above), is added to the values from the earlier years.

[31] All NADW components show a significant modification both in volume and C_{ant} inventory in the northwestern subpolar Atlantic between 1997 and 2003 (Figure 9; the boundaries of the northwestern region are indicated in Figure 9b). Only the Subpolar Mode Water (SPMW) located above the NADW remains almost unchanged. The volume of NADW in the region is affected by variability of import and export as well as in water mass formation. Figure 9 reflects the findings on the variability of LSW/ULSW formation at the end of the 1990s [*Kieke et al.*, 2007]: No LSW formation has been observed since 1997, but large amounts of the lighter ULSW have been formed between 1997 and 2003, partially replacing the LSW. Since the LSW export from the subpolar northwest Atlantic is still in process, the LSW reservoir drains. The lower boundary between LSW and NEADW is therefore rising, which explains the volume increase of the latter water mass. The DSOW is unaffected by the water mass formation processes in the Labrador Sea, and the small volume decrease may be

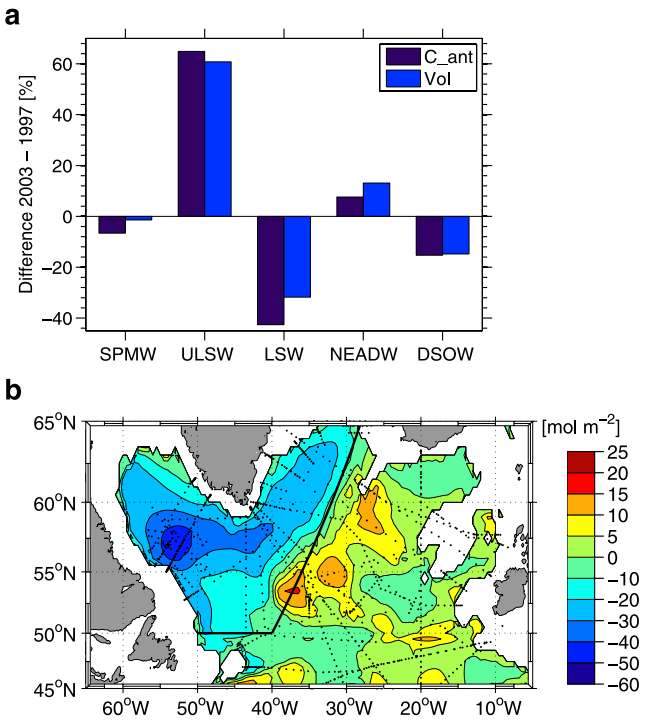

Figure 9. (a) Relative changes of volume and C_{ant} inventory (all values time-corrected toward 2003) between 1997 and 2003 within the northwest Atlantic. In the case of a steady state ocean, both differences should be zero. (b) Changes of C_{ant} column inventory (2003–1997; the 1997 values are time-corrected toward 2003) for LSW. The northwest Atlantic region is limited by the bold black line.

due to reduced import from the Denmark Strait between Greenland and Iceland [*Macrander et al.*, 2005].

[32] The variability of the C_{ant} inventories of the different water masses is dominated by their volume changes (Figure 9a). For LSW and NEADW, the C_{ant} decrease even exceeds the volume reduction. This can be explained by the "aging" of water. In the absence of ventilation and/or advection of younger water, as was the case for LSW, the water becomes older and the C_{ant} concentration remains constant. The aging thus leads to a reduction of the time-corrected C_{ant} inventory. For LSW, this effect makes up about 11%, which is exactly the expected temporal increase. This means that for LSW in 2003 the mean C_{ant} concentration is the same as in 1997. For NEADW, the difference is about 8%, which implies an increase of the (mean) C_{ant} concentration of 3%, instead of 11% that would result from a constant water mass age. The NEADW receives some of its C_{ant} content by vertical mixing with LSW and is also influenced by the aging of this water mass. Over the whole water column, the C_{ant} inventory in the western subpolar North Atlantic increased only by 2% between 1997 and 2003 (or decreased by 9% if the 1997 data are time-corrected), much less than the 11% that would be expected from the rising atmospheric CO_2 levels. This corresponds to a C_{ant} deficit of 0.2 ± 0.1 Pg C.

[33] The correlation between LSW formation and C_{ant} inventory changes is also reflected by the spatial distribution of the C_{ant} column inventories. The first half of the 1990s are characterized by high LSW formation rates. In 1997, large portions of this newly formed LSW are still present in the Labrador and Irminger Sea. Thus the LSW C_{ant} column inventory is extraordinary high in the subpolar northwest Atlantic in 1997 and decreases afterward. In 2003, parts of the LSW formed prior to 1997 have been exported into the northeast Atlantic. This leads to the observed changes of the C_{ant} inventory of LSW in the North Atlantic, i.e., a decrease in the western and an increase in the eastern part (Figure 9b). In this manner, the decreasing LSW volume and C_{ant} inventory over the western subpolar North Atlantic is partially compensated by an increase in the eastern region. The influence of the cessation of LSW formation for the Atlantic C_{ant} inventory is thus minimized, but will be enhanced once all the LSW has left the western and eastern subpolar North Atlantic.

6. Discussion

[34] The inventory of anthropogenic carbon is calculated for the Atlantic between 20°S and 65°N with the TTD method using two sets of CFC data collected around 1997 and 2003. The C_{ant} inventory is 32.5 ± 9.5 Pg C in 1997 and 36 ± 10.5 Pg C in 2003. The inventory increase is in agreement with the rising atmospheric CO_2 and C_{ant} concentrations in the surface mixed layer; thus no influence of ocean variability on the C_{ant} storage for the whole region between 20°S and 65°N can be observed.

[35] The C_{ant} inventories calculated here illustrate the important role of the Atlantic for the global C_{ant} uptake. The region of the Atlantic between 20°S and 65°N makes up only 14% of the area of the world ocean, but stores about 25% of the oceanic anthropogenic carbon. The resulting accumulation rate is 0.55 Pg C a^{-1}. This value is considerably larger than the C_{ant} accumulation rate calculated by [*Quay et al.*, 2007] from $\delta^{13}C$ data for the North Atlantic of 0.32 Pg C a^{-1}. On the other hand, *Friis et al.* [2005] gives a change of the C_{ant} storage of 0.27 Pg C a^{-1} for the region north of 40°N over the period 1981–1997, which exceeds the results from this study of 0.16 Pg C a^{-1} for the same region.

[36] The C_{ant} accumulation rate of 0.55 Pg C a^{-1} calculated here is in agreement with an earlier study based on CFC ages [*McNeil et al.*, 2003] and the climatological carbon uptake for the North Atlantic [*Takahashi et al.*, 2002]. The latter value, however, is the carbon uptake by air-sea exchange only and also includes natural carbon. The C_{ant} inventory of the Atlantic between 20°S and 65°N also increases because of advection of C_{ant}. The northward upper branch of the Meridional Overturning Circulation carries C_{ant} rich waters northward at 20°S, whereas the export of C_{ant} due to the southward flowing NADW is smaller.

[37] The inventories calculated here can be compared with results from previous studies by *Sabine et al.* [2004] based on the ΔC^* method and by *Waugh et al.* [2006] based on the TTD method. In these studies, C_{ant} is calculated for 1994. For comparison, Table 2 shows the C_{ant} inventory for the different studies calculated in the same latitude bands for 1994 (the 1997 data from this study are reduced by the

annual increase of 1.69% a^{-1}). The values from this study are slightly higher for the subpolar and subtropical region. The disagreement, however, is much smaller than the methodological error discussed in section 4.2. The similar column inventories for the different methods used in the different studies, however, are partly due to compensating errors. Relatively low values in the deep waters for the ΔC^* method are opposed to higher values in the upper ocean [*Waugh et al.*, 2006; *Tanhua et al.*, 2007]. The earlier TTD study from *Waugh et al.* [2006] uses a fixed ratio of $\Delta/\Gamma = 1$. The variable Δ/Γ applied here is typically smaller than one in the subpolar and larger than one in the tropical Atlantic (Figure 3b). As C_{ant} decreases with increasing Δ/Γ, this may explain the differences of the C_{ant} inventory in the northern and southern region between this study and the earlier one.

[38] *Lee et al.* [2003] calculated the C_{ant} inventory for the Atlantic in the same way as *Sabine et al.* [2004], but the values are given within 10° latitude bands and are divided between the western and eastern basin of the Atlantic. These mean column inventories are compared with the results from this study (Figure 10). In the eastern basin the agreement is quite good, whereas the values derived here are larger in the western basin, especially in the subpolar region. This again indicates that the ΔC^* method gives less C_{ant} in the recently ventilated deep (overflow) waters, which spread southward mainly in the western basin of the Atlantic, especially the DWBC. Further investigations are thus necessary to reconcile the C_{ant} inventory of the different methods, which have been analyzed by *Vázquez-Rodriguez et al.* [2009], and to exactly quantify the role of the deep oceans for the C_{ant} storage.

[39] A number of model studies suggest a significant reduction of deep water formation rates in the North Atlantic may occur as a consequence of global warming [*Schwekendiek and Willebrand*, 2005; *Stouffer et al.*, 2006]. As more than 40% of the Atlantic C_{ant} inventory are taken up by NADW, the extreme scenario of a complete shutdown of NADW formation would reduce the annual C_{ant} uptake from 0.55 to 0.3 Pg C a^{-1}, i.e., by more than 10% of the global C_{ant} uptake rate of 2.2 Pg C a^{-1} [*Takahashi et al.*, 2002]. The observed decline of the C_{ant} storage over the subpolar North Atlantic between 1997 and 2003 corresponds to a decrease of oceanic carbon uptake of only 0.033 Pg C a^{-1}. This result supports the finding from a study based on a coarse resolution physical-biogeochemical climate model [*Joos et al.*, 1999], where larger reductions in the oceanic C_{ant} inventory of the order of 10% or more only occur for the case of a total shutdown of the Meridional Overturning Circulation. *Schuster and Watson* [2007] calculated an integrated decrease of the carbon sink over the North Atlantic of 0.24 Pg C a^{-1}, much larger than the small decrease found here. One reason is that the flux study of *Schuster and Watson* [2007] contains natural carbon as well, whereas here only C_{ant} changes, which are due to changes in the solubility pump, are considered.

Table 2. Comparison of C_{ant} Inventories in Pg C for Different Latitude Bands of the Atlantic in 1994

	Sabine et al. [2004]	*Waugh et al.* [2006]	This Study
50°–65°N	4	4	5
14°–50°N	16	17	18
14°S–14°N	7	8	7

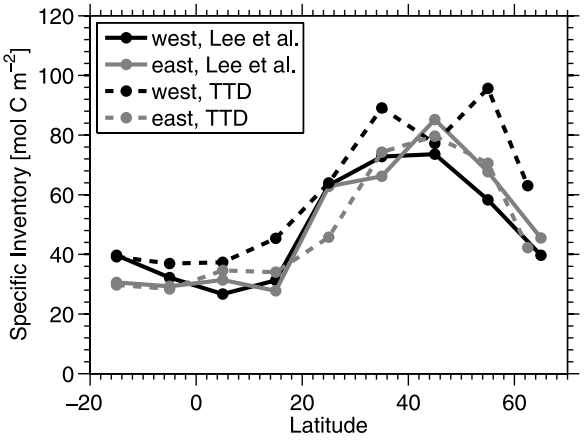

Figure 10. Specific inventory of C_{ant} for the west and east Atlantic in 10° latitude bands in 1994 from *Lee et al.* [2003] and this study (TTD).

[40] The situation in 1997, with a large LSW reservoir in the subpolar region, was an exception favored by the long positive North Atlantic Oscillation (NAO+) period from 1988 to 1996. *Tait et al.* [2000] have already shown that C_{ant} in the Labrador Sea in the LSW increased between 1993 and 1995 and remained almost constant between 1995 and 1997 because of the stop of deep convection. Here we demonstrated that this trend continued and the C_{ant} concentration in LSW remained constant until 2003 because of the aging of this water mass. The C_{ant} inventory in LSW in the north western Subpolar Atlantic decreased because of the export of this water mass. Similar results are found in the work of *Pérez et al.* [2008] along a section in the Irminger Sea: A large C_{ant} increase during the early 1990s is followed by a period of reduced C_{ant} uptake from 1997 onward. At present, it is not clear whether the decline of LSW formation and C_{ant} storage in the western subpolar North Atlantic is already a signal of long-term climate change. Longer observational time series are necessary in order to detect a possible decline of oceanic C_{ant} uptake due to global warming.

[41] **Acknowledgments.** We thank the captain, crews, and scientists of the various cruises, especially the PIs who made their data public. We acknowledge the provision of recent CFC data by R. Fine and W. Smethie for the analysis. This study was funded by the EU in the framework of CARBOOCEAN, project 511176 (GOCE).

References

Anderson, L. A. A., and J. L. Sarmiento (1994), Redfield ratios of remineralization determined by nutrient data analysis, *Global Biogeochem. Cycles*, *8*(1), 65–80.

Corbière, A., N. Metzl, G. Reverdin, C. Brunet, and T. Takahashi (2006), Interannual and decadal variability of the oceanic carbon sink in the North Atlantic subpolar gyre, *Tellus, Ser. B*, *59*, 168–178, doi:10.111/j.1600-0889.2006.00232.x.

Dickson, A. G., and C. Goyet (Eds.) (1994), Handbook of methods for the analysis of the various parameters of the carbon dioxide system in sea

water, version 2, *ORNL/CDIAC-74*, Carbon Dioxide Inf. Anal. Cent., Oak Ridge Natl. Lab., U.S. Dept. of Energy, Oak Ridge, Tenn.

Dreisigacker, E., and W. Roether (1978), Tritium and ^{99}Sr in North Atlantic surface water, *Earth Planet. Sci. Lett.*, *38*, 301–312.

Fleischmann, U., H. Hildebrandt, A. Putzka, and R. Bayer (2001), Transport of newly ventilated deep water from the Iceland Basin to the West European Basin, *Deep Sea Res., I*, *48*, 1793–1819.

Friis, K., A. Körtzinger, J. Pätsch, and D. W. R. Wallace (2005), On the temporal increase of anthropogenic CO_2 in the subpolar North Atlantic, *Deep Sea Res., I*, *52*, 681–698.

Gammon, R. H., J. Cline, and D. Wisegarver (1982), Chlorofluoromethanes in the northeast Pacific Ocean: Measured vertical distributions and application as transient tracers of upper ocean mixing, *J. Geophys. Res.*, *87*(C12), 9441–9454.

Gruber, N., J. L. Sarmiento, and T. F. Stocker (1996), An improved method for detecting anthropogenic CO_2 in the oceans, *Global Biogeochem. Cycles*, *10*(4), 809–837.

Joos, F., G.-K. Plattner, T. F. Stocker, O. Marchal, and A. Schmittner (1999), Global warming and marine carbon cycle feedbacks on future atmospheric CO_2, *Science*, *284*, 464–467, doi:10.1126/science.284.5413.464.

Keeling, C. D., and T. P. Whorf (2005), Atmospheric CO_2 records from sites in the SIO air sampling network, in *Trends: A Compendium of Data in Global Change*, Carbon Dioxide Inf. Anal. Cent., Oak Ridge Natl. Lab., U.S. Dept. of Energy, Oak Ridge, Tenn.

Kieke, D., M. Rhein, L. Stramma, W. M. Smethie, D. A. LeBel, and W. Zenk (2006), Changes in the CFC Inventories and Formation Rates of Upper Labrador Sea Water, 1997–2001, *J. Phys. Oceanogr.*, *36*, 64–86.

Kieke, D., M. Rhein, L. Stramma, W. M. Smethie, J. L. Bullister, and D. A. LeBel (2007), Changes in the pool of Labrador Sea Water in the subpolar North Atlantic, *Geophys. Res. Lett.*, *34*, L06605, doi:10.1029/2006GL028959.

Lazier, J., R. Hendry, A. Clarke, I. Yashayaev, and P. Rhines (2002), Convection and restratification in the Labrador Sea, 1990–2000, *Deep Sea Res., I*, *49*, 1819–1835.

Lee, K., et al. (2003), An updated anthropogenic CO_2 inventory in the Atlantic Ocean, *Global Biogeochem. Cycles*, *17*(4), 1116, doi:10.1029/2003GB002067.

Lee, K., L. T. Tong, F. J. Millero, C. L. Sabine, A. G. Dickson, C. Goyet, G.-H. Park, R. Wanninkhof, R. A. Feely, and R. M. Key (2006), Global relationships of total alkalinity with salinity and temperature in surface waters of the world's oceans, *Geophys. Res. Lett.*, *33*, L19605, doi:10.1029/2006GL027207.

Lefèvre, N., A. J. Watson, A. Olsen, A. F. Rios, F. Pérez, and T. Johannessen (2004), A decrease in the sink for atmospheric CO_2 in the North Atlantic, *Geophys. Res. Lett.*, *31*, L07306, doi:10.1029/2003GL018957.

Macrander, A., U. Send, H. Valdimarsson, S. Jónsson, and R. H. Käse (2005), Interannual changes in the overflow from the Nordic Seas into the Atlantic Ocean through Denmark Strait, *Geophys. Res. Lett.*, *32*, L06606, doi:10.1029/2004GL021463.

McNeil, B. I., R. J. Matear, R. M. Key, J. L. Bullister, and J. Sarmiento (2003), Anthropogenic CO_2 uptake by the oceans based on the global chlorofluorocarbon data set, *Science*, *299*, 235–239, doi:10.1126/science.1077429.

Neftel, A., H. Friedli, E. Moor, H. Lotscher, H. Oeschger, U. Siegenthaler, and B. Stauffer (1994), Historical CO_2 record from the Siple Station Ice Core, in *Trends: A Compendium of Data in Global Change*, Carbon Dioxide Inf. Anal. Cent., Oak Ridge Natl. Lab., U.S. Dept. of Energy, Oak Ridge, Tenn.

Omar, A. M., and A. Olsen (2006), Reconstructing the time history of the air-sea CO_2 disequilibrium and its rate of change in the eastern subpolar North Atlantic, 1972–1989, *Geophys. Res. Lett.*, *33*, L04602, doi:10.1029/2005GL025425.

Pérez, F. F., M. Vázquez-Rodriguez, E. Louarn, X. A. Padin, H. Mercier, and A. F. Ríos (2008), Temporal variability of the anthropogenic CO_2 storage in the Irminger Sea, *Biogeosciences*, *5*, 1669–1679.

Quay, P., R. Sonnerup, J. Stutsman, J. Maurer, A. Körtzinger, X. A. Padin, and C. Robinson (2007), Anthropogenic CO_2 accumulation rates in the North Atlantic Ocean from changes in the $_{13}C/_{12}C$ of dissolved inorganic carbon, *Global Biogeochem. Cycles*, *21*, GB1009, doi:10.1029/2006GB002761.

Rhein, M., K. Kirchner, C. Mertens, R. Steinfeldt, M. Walter, and U. Fleischmann-Wischnath (2005), Transport of South Atlantic water through the passages south of Gouadeloupe and across 16°N, 2000–2004, *Deep Sea Res., I*, *52*, 2234–2249, doi:10.1016/j.dsr.2005.08.003.

Sabine, C. L., et al. (2004), The oceanic sink for anthropogenic CO_2, *Nature*, *305*, 367–371.

Schuster, U., and A. J. Watson (2007), A variable and decreasing sink for atmospheric CO_2 in the North Atlantic, *J. Geophys. Res.*, *112*, C11006, doi:10.1029/2006JC003941.

Schwekendiek, U., and J. Willebrand (2005), Mechanisms affecting the overturning response in global warming simulations, *J. Clim.*, *18*, 4925–4936.

Steinfeldt, R., and M. Rhein (2004), Spreading velocities and dilution of North Atlantic Deep Water in the tropical Atlantic based on CFC time series, *J. Geophys. Res.*, *109*, C03046, doi:10.1029/2003JC002050.

Steinfeldt, R., M. Rhein, and M. Walter (2007), NADW transformation at the western boundary between 66°W/20°N and 60°W/10°N, *Deep Sea Res., I*, *54*, 835–855, doi:10.1016/j.dsr.2007.03.004.

Stouffer, R. J., et al. (2006), Investigating the causes of the response of the thermohaline circulation to past and future climate changes, *J. Clim.*, *19*, 1365–1387.

Stramma, L., D. Kieke, M. Rhein, F. Schott, I. Yashayaev, and K. P. Koltermann (2004), Deep water changes at the western boundary of the subpolar North Atlantic during 1996 to 2001, *Deep Sea Res., I*, *51*, 1033–1056.

Tait, V. K., R. M. Gershey, and E. P. Jones (2000), Inorganic carbon in the Labrador Sea: Estimation of the anthropogenic component, *Deep Sea Res., I*, *47*, 295–308.

Takahashi, T., et al. (2002), Global sea-air CO_2 flux based on climatological surface, ocean pCO_2, and seasonal biological temperature effects, *Deep Sea Res., II*, *49*, 1601–1622.

Tanhua, T., A. Körtzinger, K. Friis, D. W. Waugh, and D. W. R. Wallace (2007), An estimate of anthropogenic CO_2 inventory from decadal changes in oceanic carbon content, *Proc. Natl. Acad. Sci. U. S. A.*, doi:10.1073/pnas.0606574104.

Tanhua, T., D. W. Waugh, and D. W. R. Wallace (2008), Use of SF_6 to estimate anthropogenic CO_2 in the upper ocean, *J. Geophys. Res.*, *113*, C04037, doi:10.1029/2007JC004416.

Terenzi, F., T. M. Hall, S. Khatiwala, C. B. Rodehacke, and D. A. LeBel (2007), Uptake of natural and anthropogenic carbon by the Labrador Sea, *Geophys. Res. Lett.*, *34*, L06608, doi:10.1029/2006GL028543.

Vázquez-Rodriguez, M., F. Touratier, C. LoMonaco, D. W. Waugh, X. A. Padin, R. G. J. Bellerby, C. Goyet, N. Metzl, A. F. Ríos, and F. F. Pérez (2009), Anthropogenic carbon distributions in the Atlantic Ocean: Data-based estimates from the Arctic to the Antarctic, *Biogeosciences*, *6*, 439–451.

Walker, S. J., R. F. Weiss, and P. K. Salameh (2000), Reconstructed histories of annual mean atmospheric mole fraction for the halocarbons CFC-11, CFC-12 CFC-113 and carbon tetrachloride, *J. Geophys. Res.*, *105*, 14,285–14,296.

Warner, M. J., and R. F. Weiss (1985), Solubilities of chlorofluoromethanes 11 and 12 in water and seawater, *Deep Sea Res.*, *32*, 1485–1497.

Waugh, D. W., T. W. N. Haine, and T. M. Hall (2004), Transport times and anthropogenic carbon in the subpolar North Atlantic Ocean, *Deep Sea Res. I*, *51*, 1475–1491, doi:10.1016/j.dsr.2004.06.011.

Waugh, D. W., T. M. Hall, B. I. McNeil, R. Key, and R. J. Matear (2006), Anthropogenic CO_2 in the oceans estimated using transit time distributions, *Tellus, Ser. B*, *58*, 376–389, doi:10.1111/j.1600-0889.2006.00222.x.

Weiss, R. F. (1974), Carbon dioxide in water and seawater: The solubility of a non ideal gas, *Mar. Chem.*, *2*, 203–215.

J. L. Bullister, Pacific Marine Environmental Laboratory, NOAA, NOAA Building 3, 7600 Sand Point Way NE, Seattle, WA 98115-0007, USA. (john.l.bullister@noaa.gov)

M. Rhein and R. Steinfeldt, Institut für Umweltphysik, Universität Bremen, Otto-Hahn-Allee, D-28359 Bremen, Germany. (mrhein@physik.uni-bremen.de; rsteinf@physik.uni-bremen.de)

T. Tanhua, Marine Biogeochemie, Leibniz-Institut für Meereswissenschaften an der Universität Kiel, Dsternbrooker Weg 20, D-24105 Kiel, Germany. (ttanhua@ifm-geomar.de)